HHS Public Access

Author manuscript

Endocr Relat Cancer. Author manuscript; available in PMC 2023 December 06.

Published in final edited form as:

Endocr Relat Cancer. 2023 December 01; 30(12): . doi:10.1530/ERC-23-0062.

Mammary gland development and EDC-driven cancer susceptibility in mesenchymal ERα knockout mice

Clarissa Wormsbaecher[1,2], **Brittney M. Cumbia**[2], **Emma G. Amurgis**[2], **Jillian M. Poska**[1,2], **Madeline R. Price**[1,2], **Xiaokui M. Mo**[3], **Sue E. Knoblaugh**[4], **Takeshi Kurita**[2,5], **Craig Joseph Burd**[1,2]

[1]Department of Molecular Genetics, The Ohio State University, 920 Biomedical Research T ower, 460 W. 12th Ave., Columbus, OH, 43210, USA

[2]The Ohio State University Comprehensive Cancer Center, Columbus, OH, 43210, USA

[3]Center for Biostatistics, Department of Biomedical Informatics, The Ohio State University Wexner Medical Center, Columbus, OH 43210, USA

[4]Department of Veterinary Biosciences, The Ohio State University, Columbus, OH, 43210, USA

[5]Department of Cancer Biology and Genetics, The Comprehensive Cancer Center, The Ohio State University, Columbus, OH, 43210, USA

Abstract

Development of the mammary gland requires both proper hormone signaling and crosstalk between the stroma and epithelium. While estrogen receptor (ERα) expression in the epithelium is essential for normal gland development, the role of this receptor in the stroma is less clear. Moreover, several lines of evidence suggest that mouse phenotypes of in utero exposure to endocrine disruption act through mesenchymal ERα in the developing fetus. We utilized a Twist2-cre mouse line to knockout mesenchymal ERα. Herein, we assessed mammary gland development in the context of mesenchymal ERα deletion. We also tested the effect of in utero BPA exposure to alter the tumor susceptibility in the MMTV-neu breast cancer mouse model. Mesenchymal ERα deletion resulted in altered reproductive tract development and atypical cytology associated with estrous cycling. The mammary gland demonstrated mature epithelial extension unlike complete ERα knockout mice, but ductal extension was delayed and reduced compared to ERα-competent mice. Using the MMTV-Neu cancer susceptibility model, ERα intact mice exposed to BPA had reduced tumor free survival and overall survival compared to BPA-exposed mice having mesenchymal ERα deletion. This difference is specific for BPA exposures as vehicle treated animals had no difference in tumor development between mice expressing and not expressing mesenchymal ERα. These data demonstrate that mesenchymal ERα expression is not required for ductal extension, nor does it influence cancer risk in this mouse model, but does influence the cancer incidence associated with in utero BPA exposures.

Corresponding author: Craig J. Burd, 920 Biomedical Research Tower, 460 W. 12th Ave. Columbus, OH 43210. craig.burd@osumc.edu.

Declaration of Interest

There are no conflicts of interest that would affect the impartiality of this research.

Keywords

Endocrine disruptors; mammary gland; estrogen receptor; MMTV-Neu

Introduction

Estrogen receptor alpha (ERα) is required for full mammary gland development. ERα knockout mice have mammary glands that appear normal at birth but fail to mature. Specifically, adult ERα knockout mice have a primitive ductal rudiment at four months of age and lack terminal end buds or alveolar development (Korach et al., 1996, Bocchinfuso and Korach, 1997, Mallepell et al., 2006). ERα signaling is thus required for full mammary gland development and it drives adolescent branching, proliferation of epithelial cells, and ductal growth (Korach et al., 1996, Bocchinfuso and Korach, 1997, Mallepell et al., 2006, Sternlicht, 2006).

Initial tissue recombination and transplant experiments demonstrated a requirement of stromal ERα expression for proper epithelial ductal growth, while epithelial deletion could be overcome with high levels of hormone (Feng et al., 2007, Mueller et al., 2002, Cunha et al., 1997). It has since been shown mice in these experiments did not have full ERα deletion, but instead were hypomorphic retaining some receptor function (Kos et al., 2002, Couse et al., 1995). Conditional ERα deletion in the epithelium later demonstrated that receptor expression is also mandatory in the epithelium (Feng et al., 2007). Due to the caveats of the original tissue recombination experiments, the precise role of ER in the stroma is still unclear.

Adding to the intricacies of cell type specific ERα signaling in the mammary gland is the known risk of inappropriate estrogen signaling during fetal development in both humans and mice. In mice, ERα is expressed in the mammary mesenchyme in utero (Hindman et al., 2017, Robinson, 2007, Parmar and Cunha, 2004), while ERα begins to be expressed in the epithelium three days after birth (Haslam and Nummy, 1992). In contrast to mice, the developing human mammary gland begins to express ERα at 30 weeks of gestation (Keeling et al., 2000, Naccarato et al., 2000, Friedrichs et al., 2007). ERα expression has not been reported in utero in the mammary mesenchyme, however analysis between 7–14 weeks of gestation is extremely limited (Keeling et al., 2000, Naccarato et al., 2000, Friedrichs et al., 2007). That period corresponds to when mouse ERα expression is concentrated in the mesenchyme surrounding the epithelial bud (Hindman et al., 2017). Highlighting the importance of that time frame, data in mice (Hindman et al., 2017) suggested that this period (e11.5–14.5) is most susceptible to BPA-induced phenotypes. Observations in DES-exposed daughters suggest that first trimester exposures to endocrine disrupting compounds (EDCs) are most critical for cancer risk in line with the 7–14 week period in which the epithelial bud is surrounded by the primordial mesenchyme (Hatch et al., 1998, Hoover et al., 2011, Palmer et al., 2006). Rodent studies of in utero endocrine disruption correlated bisphenol a (BPA) actions to estrogen receptor alpha (ERα) signaling (Wadia et al., 2013, Weber Lozada and Keri, 2011, Hindman et al., 2017, Speroni et al., 2017, Soto et al., 2013). Further connecting BPA actions to mesenchymal targets, we have shown that BPA

induces transcriptional reprogramming of fibroblasts associated with known cancer-driving phenotypes (Wormsbaecher et al., 2020). Taken together, these data suggest that the risks and phenotypes could be due to BPA signaling through mesenchymal ERα (Hindman et al., 2017, Soto et al., 2013, Speroni et al., 2017, Weber Lozada and Keri, 2011, Wadia et al., 2013). However, the inability to genetically test this hypothesis due to ERα knockout mammary gland defects has resulted in a gap in the field.

In this study, we generated a mesenchymal ERα knockout mouse and assessed the development of the mammary gland and reproductive tract. Further, we investigated BPA-associated tumorigenesis by crossing the mesenchymal ERα knockout into the MMTV-neu breast cancer mouse model.

Materials and Methods

Mice

All animal research as performed in compliance with protocols approved by The Ohio State University Institutional Animal Care and Use Committee (IACUC, Protocol #2013A00000030) and in accordance with the Animal Research: Reporting of In Vivo Experiments (ARRIVE) guidelines. To generate mesenchymal ERα knockout mice (further referred to as ERαΔM), *Esr1* (ERα) floxed mice were crossed to *Twist2*-cre mice (B6.129X1-Twist2tm1.1(cre)Dor/J;JAX stock #008712) (Šošić et al., 2003) and backcrossed six generations to the FVB/NJstrain. ERα floxed mice were a kind gift from the lab of Sohaib Khan (Feng et al., 2007). ERαΔM mice were crossed to the MMTV-neu(FVB/N-Tg(MMTVneu)202Mul/J;JAX stock #002376) breast cancer mouse model (further referred to as ERαΔM-MMTV-neu) (Muller et al., 1996, Guy et al., 1992). All mice were maintained in polysulfone cages and fed a diet containing minimal levels of phytoestrogens (Harlan2019X).

For experimental studies, $Esr1^{fl/fl}$/$MMTVneu^{+/+}$$Cre^{-/-}$ females were bred with $Esr1^{fl/fl}$/$MMTVneu^{+/+}$/$Cre^{+/-}$ males to produce both mesenchymal ERα intact and deficient littermates. For endocrine disruption experiments, BPA was dissolved in sesame oil and administered to pregnant mice via oral gavage at 25 ug/kg · bodyweight (≥99%) from embryonic day 9.5 through 18.5 (E9.5-E18.5). This BPA dose has previously shown to be relevant to human exposures and result in EDC-driven mammary at these time points (Hindman et al., 2017, Wormsbaecher et al., 2020).

Tissue harvesting and preparation

To confirm mesenchymal ERα knockout, embryos were harvested at embryonic day 13.5 (E13.5) as previously described (Hindman et al., 2017). Briefly, the embryos were fixed for 48 hours in 10% neutral buffered formalin and then transferred to 70% ethanol before being embedded in paraffin for immunohistochemistry. To exclude males and only include females in analysis, the sex of the fetal tissue was determined by PCR using primers for the Y chromosome [F: TGAGTAGAGCAGTTACCTTCAATTAG, R: GTACTTCTGAGTTCTGGACACTTT, expected product size 453 base pairs]. Additionally, these mice were genotyped for ERα status [ERα flox F:

TGGGTTGCCCGATAACAATAAC, ERα flox R: AAGAGATGTAGGGCGGGAAAAG, ESR1 flox R: ACACATGCAGCAGAAGGTATTTGC, expected product sizes 356, 400, and/or 600 base pairs] (ERα flox F and ERα flox R primers from (Feng et al., 2007)) and *Twist2*-cre status [Twist2-cre Mutant F: AACTTCCTCTCCCGGAGACC, Twist2-cre Mutant R: CCGGTTATTCAACTTGCACC, Twist2-cre Wild Type F: CGTCTCAGCTACGCCTTCTC, Twist2-cre Wild Type R: TCACGAGGAGAGATACACTGG] (primer sequences from Jackson Labs JAX stock #008712).

The ERαΔM-MMTV-neu mice and control were characterized at pubertal (4.7 weeks) and adult (12–14 or 30 weeks) time points. Mice were genotyped for ERα status, *Twist2*-cre status, and MMTV-neu status [F:TCCGGAACCCACATCAGGC, R:GTTTCCTGCAGCAGCCTACGC]. For each mouse, one fourth inguinal gland was collected for whole mount analysis and the other gland was fixed for 48 hours in 10% neutral buffered formalin and then transferred to 70% ethanol before being embedded in paraffin for immunohistochemistry (Hindman et al., 2017). The tissue was cut in 6 mM thick sections.

At the adult timepoints, the estrous cycle of the mice was monitored by vaginal cytology (Hindman et al., 2017, Westwood, 2008, Byers et al., 2012, Cora et al., 2015, Caligioni, 2009), images were taken under 20X magnification. Mammary glands were harvested in the diestrus stage, unless otherwise noted in text and/or figure legend. Additionally, the female reproductive tract (ovaries, uterus, vagina) was harvested. Hematoxylin and eosin (H&E) stained reproductive tract was used to confirm the mice were in diestrus or estrus stage (Byers et al., 2012, Caligioni, 2009). H&E vaginal images were taken under 20X magnification.

Fetal immunohistochemistry (IHC) and analysis

To detect ERα expression in the mammary mesenchyme, IHC for ERα was performed on the embryos collected at E13.5. Paraffin embedded tissue sections were rehydrated and then subjected to heat mediated antigen retrieval in citrate buffer (Dako S1699) for 30 minutes. Samples were allowed to cool to room temperature for 20 minutes, then underwent blocking to prevent endogenous background staining. Tissue was incubated with 3% H_2O_2 for 15 minutes. Then tissue was incubated with Dako protein block (Dako X0909) and then avidin and biotin block (Vector Laboratories SP2001). Next, tissue was incubated with ERα antibody (Abcam ab32063, 1:4000) diluted in antibody diluent (Dako S0809). Subsequent detection occurred using biotinylated secondary antibody (IHC select 21537), R.T.U. Vectastain kit all-in-one ABC reagent (PR-7100), and DAB (Agilent K3468). Then slides were counterstained with hematoxylin, dehydrated, and mounted. Images were taken under 20X magnification.

Mammary, reproductive tract, and tumor IHC and analysis

IHC was performed for dual ERα/α-smooth muscle actin (α-SMA), progesterone receptor (PR)/α-SMA, Ki67/ α-SMA, and keratin 14/ cytokeratin 8 following the same protocol as above for the fetal IHC, with minor modifications. Heat mediated antigen retrieval

in citrate buffer (Dako S1699) occurred for 45 minutes, followed by cooling to room temperature for 30 minutes. Following protein block, tissue was incubated with either ERα (Abcam ab32063 at 1:2000), PR (Dako A0098, 1:500), Ki67 (Abcam ab16667, 1:200) or keratin 14 (Biolegend 905301, 1:5000). Mammary sections following DAB staining were blocked for 20 minutes in ready-to-use 2.5% horse serum (Vector ImmPRESS kit MP-5401). Tissues were incubated with the correlating second primary antibody; either α-SMA (Sigma SAB5500002, 1:200) (for ERα, PR, and Ki67) or cytokeratin 8 (Abcam ab59400, 1:2000). Subsequent detection occurred using the AP-Polymer ImmPRESS-AP Reagent (Vector ImmPRESS kit MP-5401) and liquid fast red substrate system (Abcam ab64254). Then slides were counterstained with hematoxylin, dehydrated, and mounted. In the reproductive tract, ERα staining was detected with Alexa-Fluor488 anti-rabbit IgG (H+L) (1:100, 711–546-152, Jackson ImmunoResearch Laboratories, West Grove, PA) and nuclei stained with Hoechest 33258 (1:10000, Sigma-Aldrich, St. Louis, MO).

Adult mammary glands were analyzed by taking six representative images of ducts in each gland (and averaged per mouse) at 20X magnification with the Vectra Automated Multispectral imaging system. Quantification of IHC was performed using the inForm Advanced Image Analysis Software, version 2.6, (Akoya Biosciences Hopkinton, MA) as previously described with minor modifications (Hindman et al., 2017). Manual tissue compartment segmentation was used to separate epithelial and stromal compartments, using α-SMA staining as designation of the epithelial compartment. In the epithelial compartment, adaptive cell segmentation and hematoxylin counter stain was used for cell/ nuclei identification. In the stromal compartment, cell segmentation and hematoxylin counter stained was used for cell identification. Scoring occurred using 2-bin positivity to identify DAB signal as positive staining (for either ERα, PR, or Ki67 IHC) and a threshold was set to differentiate between DAB positive and DAB negative (H&E only) stained cells/ nuclei. Scoring for the epithelial and stromal compartments was performed separately and the threshold set for each compartment was applied to each image.

Tumor Ki67 positivity was averaged over six images at the edges of each tumor at 20X magnification with the Vectra Automated Multispectral imaging system. Quantification of tumor IHC was performed using the QuPath-0.3.2 Software (Bankhead et al., 2017). The StarDist extension was used for cell segmentation to identify cells/ nuclei by recognizing hematoxylin counter stain and for positivity threshold setting to determine DAB positive (Ki67) and DAB negative (H&E only) stained cells/ nuclei. Positivity is shown as percent of positive cells compared to the total cell count.

Mammary whole mounts and analysis

Mammary whole mounts were carmine aluminum stained using the National Toxicology Program Animal Studies Protocol, Section XIII, Appendix 6, Section E) (2011). The whole mounts collected at 4.7 weeks were imaged using a dissection microscope at 1X magnification and analyzed for epithelial elongation, as previously described (Hindman et al., 2017). Terminal endbuds were quantified as distal structures that measured twice as wide as the leading duct (Matouskova et al., 2022). The whole mounts collected at the adult time point between 12–14 weeks were imaged using a dissection microscope at 0.6X

magnification and analyzed for epithelial area (Hindman et al., 2017, Stanko et al., 2015). Images were de-identified and analyzed blind to the experimental conditions. Scholl analysis of whole mount images was performed as previously described (Stanko and Fenton, 2017).

Serum collection and analysis

Blood samples were collected in EDTA coated tubes and serum was collected following the recommended instructions from The University of Virginia Center for Research in Reproduction Ligand Assay and Analysis Core. Samples were allowed to clot at room temperature for 90 minutes followed by centrifugation at 2000 x g for 15 minutes at room temperature. Serum was removed and stored at −20°C before analysis for estradiol and progesterone levels at The University of Virginia Center for Research in Reproduction Ligand Assay and Analysis Core. The University of Virginia Center for Research in Reproduction Ligand Assay and Analysis Core is supported by the Eunice Kennedy Shriver NICHD/NIH Grant R24HD102061.

Tumor monitoring

Following in utero exposure, female mice were allowed to age and monitored twice per week for tumor formation, while blind to genotype and treatment. Established mammary tumors were measured twice per week by caliper for tumor size (width and length in mm). At the time of exclusion criteria, tumors were harvested and fixed in 10% neutral buffered formalin and embedded in paraffin for immunohistochemistry. Data graphed as Kaplan-Meier survival curves for tumor free survival (time to first tumor detection) and overall survival (time until tumor reached exclusion criteria).

Tumor histology and pathology

Four tumors per genotype/ treatment group were randomly selected and paraffin sections of 4 μm were stained with hematoxylin and eosin (H&E). H&E sections were evaluated by light microscopy (Nikon Eclipse Ci, Nikon Instruments, Melville, NY) with attached SC50 digital camera, (Olympus, B and B Microscopes Limited, Pittsburgh, PA) by a board-certified veterinary pathologist (S.E.K.) blinded to genotype and study group. Representative H&E images were taken at 10X and 20X magnification.

Statistics

Data analyses were performed using a two-sample t-test or analysis of variance (ANOVA) for experiments involved two and multiple groups, respectively. Tumor free survival and overall survival of groups were compared using log-rank test.

Results

Twist2-cre eliminates ERα expression in the embryonic mesenchyme and reduces expression in the adult stroma

Numerous studies have implicated ERα in the mesenchymal cells surrounding the developmental mammary bud as a target of in utero BPA action (Wadia et al., 2013, Speroni et al., 2017). In order to genetically test the contribution of mesenchymal ERα on in utero

EDC signaling, we crossed ERα floxed mice with mice expressing Cre recombinase under the *Twist2* promoter (ERαΔM). Twist2 is expressed in the mammary mesenchymal cells starting at embryonic day 11.5, but is more prominent between embryonic days 12.5 (E12.5) and E15.5 (Hiremath et al., 2012) which overlaps with the ERα expression we observe in the mammary mesenchymal cells (Hindman et al., 2017). To validate our knockout, we examined the expression of ERα in the developing perinatal mammary gland in our Cre-control mice and our ERαΔM mice at E13.5 (Fig. 1A). To verify mammary buds, we stained sequential sections for androgen receptor (AR) expression which is also present in the mesenchyme surrounding the mammary bud (Fig. 1A) (Dart et al., 2013). In our control sample, ERα was expressed in the mammary mesenchyme surrounding the ERα negative developing mammary epithelial bud as expected. Our ERαΔM mice have little to no visible ERα expression in the mammary mesenchyme confirming our mesenchymal ERα knockout (Fig. 1A).

As the goal of this study was to assess the requirement of mesenchymal ERα on EDC-induced increases in carcinogenesis, we crossed our ERαΔM mice to the MMTV-neu breast cancer mouse model, which are known as our ERαΔM-MMTV-neu mice. To begin to characterize the ERαΔM-MMTV-neu mice, we examined ERα expression (Fig. 1B) and PR expression (Fig. 1D) in the 12–14 week old mammary glands in the epithelial compartment and the stromal compartment surrounding the ductal epithelium. Dual IHC staining utilized α-SMA, which highlights myoepithelial cells, as a marker to differentiate the epithelial tissue compartment from the surrounding stroma. While we found no change in the ERα positivity in the epithelial compartment between the littermate Cre- control and ERαΔM-MMTV-neu mice, there was a significant decrease in ERα positivity in the stromal compartment in the ERαΔM-MMTV-neu mice (Fig. 1C). We found no change in the PR positivity in the epithelial and stromal compartments between the control and ERαΔM-MMTV-neu mice (Fig. 1E).

Mesenchymal ERα knockout mice have an altered response to estrous cycling in the reproductive tract

The morphological phenotype of the mammary glands changes with the estrous cycle and therefore we collected tissue samples synchronized to the same phase of the cycle as measured by vaginal cytology (Westwood, 2008, Byers et al., 2012, Cora et al., 2015, Caligioni, 2009). Crystal violet staining of vaginal cytology samples in ERαΔM-MMTV-neu mice displayed evidence of estrous cycling, as cytology samples were identified that represented four stages of the estrous cycle (Fig. 2A). Although cytology samples were able to be collected indicating all four stages of the estrous cycle, analysis of a large cohort of mice indicated abnormal reproductive tract phenotypes associated with estrous cycling. Most vaginal cytology samples in ERαΔM-MMTV-neu mice did not clearly match any stage, disrupting the ability to effectively stage and assess cycling accurately using vaginal flushing (Fig. 2B).

Reproductive tracts of control and ERαΔM-MMTV-neu samples were harvested and H&E staining of the reproductive tract was used to confirm estrous stage (Byers et al., 2012, Caligioni, 2009). Vaginal cytology was used to approximate estrous cycle when harvesting

ERαΔM-MMTV-neu mice for confirmation. The reproductive tract in the ERαΔM-MMTV-neu females that displayed vaginal cytology similar to estrus stage appears significantly smaller compared to the Cre- control mice (Fig. 2C, left panels). In mice, that displayed vaginal cytology approximating diestrus stage, the overall size appears similar between control and ERαΔM-MMTV-neu mice (Fig. 2C, right panels). H&E analysis of vaginal sections showed a decreased amount of stroma in the ERαΔM-MMTV-neu mice, which made stage confirmation impossible. (Fig. 2D, samples collected in estrus stage by vaginal cytology). As complete ERα results in a roughly 10 fold increase in circulating estradiol and a 2 fold increase in progesterone (Couse et al., 1995), estradiol and progesterone serum levels in the ERαΔM-MMTV-neu mice were assessed. Vaginal cytology was used to best assess the estrous stage of mice for serum collection, however due to the estrous cycle being impossible to confirm, ERαΔM-MMTV-neu samples were all grouped together and cytology approximation noted for each sample. No significant change in either circulating estrogen or progesterone was detected for ERαΔM-MMTV-neu mice. We examined the expression of ERα within the reproductive tract to determine if the phenotypes were likely driven by the inability to properly respond to hormone levels. In ERαΔM-MMTV-neu mice, ERα was heterogeneously expressed in the stroma of the vagina and uterus, indicating Twist2-cre deleted ERα in a substantial population of stromal cells (Supplemental Fig. 1). It should be noted that estrogen regulates the proliferation and differentiation of vaginal and uterine epithelial cells through the ERα in the stromal cells (Buchanan et al., 1998, Kurita et al., 2001, Cooke et al., 1997, Buchanan et al., 1999). Thus, the partial loss of stromal ERα in the female reproductive tract explains the abnormal vaginal cytology in the ERαΔM-MMTV-neu mice. Additionally, uterine epithelial PR is downregulated by estrogen action via uterine stromal ERα (Kurita et al., 2000), and the epithelial PR downregulation is crucial for embryo implantation (Wetendorf et al., 2017). Finally, ERαΔM-MMTV-neu females did not produce any litters and no plugs were observed when housed with male mice.

Mesenchymal ERα loss does not prohibit mammary gland maturation and epithelial elongation

For the majority of our analyses of mammary glands, we harvested mammary glands of our control samples in diestrus and ERαΔM-MMTV-neu samples in a stage we identified closest to diestrus based on the vaginal cytology unless otherwise noted in the text and figure legend. To assess whether knocking out mesenchymal ERα alters mammary gland development, we looked at mammary whole mounts at 4.7 weeks (puberty) (Fig. 3A) and at two adult time points of 12–14 (Fig. 3D) and 30 (Fig. 3F) weeks of age. ERαΔM-MMTV-neu mice have a statistically significant reduced epithelial elongation compared to control mice at 4.7 weeks (Fig. 3B). Interestingly, the phenotype of delayed epithelial elongation in puberty mimics the phenotype caused by in utero BPA exposure (Hindman et al., 2017). The reduced epithelial elongation is coincident with a reduced number of terminal end buds in the ERαΔM-MMTV-neu mice (Fig. 3C, Supplemental Fig. 2A). At roughly 12–14 weeks, the epithelial ducts in the ERαΔM-MMTV-neu mice extend beyond the lymph node and into the mammary fat pad but do not fill the fat pad as in the control mice (Fig. 3D). The epithelial distance from the nipple to the furthest duct end as a percentage of the distance from the nipple to end of fat gland was measured. ERαΔM-MMTV-neu mice

displayed a shorted extension than control mice (Supplemental Fig. 2B). However, scholl analysis revealed no change in branching complexity between ERαΔM-MMTV-neu mice and littermate controls (Supplemental Fig. 2C). When assessing epithelial area, we found that the ERαΔM-MMTV-neu mice have a significantly reduced amount of epithelial area (Fig. 3E). The epithelial ducts of mesenchymal ERα knockout mice at about 30 weeks of age have extended further into the fat pad, but still appear to not extend throughout the fat pad (Fig. 3F).

We examined Ki67 expression (Fig. 3G) in the adult (12–14 weeks) mammary glands in the epithelial compartment and the stromal compartment surrounding the ductal epithelium. Dual IHC staining utilized α-SMA was as a marker to differentiate the epithelial tissue compartment from the surrounding stroma. We found no change in the proliferation assessed by Ki67 positivity in either the epithelial or stromal compartment between the control and ERαΔM-MMTV-neu mice (Fig. 3G). Additionally, we used dual IHC to look at cytokeratin 8 and keratin 14 (Fig. 3H) to compare the luminal and basal epithelium, respectively (Smalley, 2010). No changes between the epithelial population in the control and mesenchymal ERα knockout mice were observed.

Mesenchymal ERα deletion delays onset of tumors following in utero BPA exposures

As females with mesenchymal ERα knockout do not produce offspring, we crossed $ERα^{fl/fl}$/MMTV-$neu^{+/+}$/*Twist2*-$Cre^{-/-}$ female mice to $ERα^{fl/fl}$/MMTV-$neu^{+/+}$/*Twist2*-$Cre^{+/-}$ male mice. Pregnant females were exposed to 25 μg/kg · bodyweight BPA or oil control from E9.5 through E18.5. We have previously shown this dose results in amniotic BPA levels comparable to reported human amniotic levels (Hindman et al., 2017). This breeding and dosing scheme allowed for comparisons between littermate controls creating 4 testing groups: 1) ERα competent/ oil treated 2) ERα competent/ BPA treated 3) ERαΔM/ oil treated 4) ERαΔM/ BPA treated. We observed no significant morphologic differences in the tumors between the four groups via evaluation of H&E stained tumor sections (Fig. 4A–B). All tumors were classified as mammary adenocarcinoma, solid subtype and showed similar histomorphology of neoplastic cells and pattern of cells. The average mitotic rate varied from 2–7 mitoses per 40X high power field. All groups and most sections evaluated had many dilated, congested vessels and large blood-filled cavities present with focal to multifocal areas of necrosis. Additionally, we found no change in the proliferation within the tumors (Fig. 4C–D).

Despite the differences in epithelial content observed between ERαΔM mice and Cre-littermate controls (Fig. 3), there was no difference in the initial detection of tumors (Fig. 4E, compare blue lines) or survival (Fig. 4F, compare blue lines) between both oil-exposed groups (control and ERαΔM-MMTV-neu). In utero BPA exposure trended to have a worse outcome with regards to tumor free survival and overall survival compared to both oil treated experimental groups (tumor free survival BPA-exposed control to oil-exposed control p=0.2820 and overall survival BPA-exposed control to oil-exposed control p=0.3394). However, when comparing BPA-exposed control to BPA-exposed ERαΔM-MMTV-neu, BPA-exposed control mice had statistically worse tumor free survival (p=0.0233) and overall survival (p=0.0343). Variation seen in littermates was comparable to variation of the at large

cohort suggesting differences were not driven by litter effects. Additionally, there was no change in tumor burden amongst the four groups (Supplemental Fig. 3).

Discussion

Role of mesenchymal ERα in mammary gland and reproductive tract development

In this study, our goal was to determine the requirement of mesenchymal ERα to drive an increase in tumorigenesis following in utero BPA exposure. In our ERαΔM-MMTV-neu model, mammary glands have delayed or reduced epithelial elongation, but do undergo epithelial extension through most of the fat pad in contrast to the full ERα knockout mouse (Korach et al., 1996, Bocchinfuso and Korach, 1997, Mallepell et al., 2006). This indicates mesenchymal ERα is not required for maturation. Interestingly, previous tissue recombination studies using subrenal transplantation into nude mice demonstrated that with neonatal wildtype mammary epithelium and neonatal ERα knockout stroma, there were an extremely small number of mammary ducts that almost went unrecognized. They concluded that stromal ERα, but not epithelial ERα, was required for full mammary ductal growth (Cunha et al., 1997). A later study moved to extrapolate these findings into mature mammary tissue by injecting wildtype epithelial cells into an ERα knockout stroma, using mice from all the same background, and the opposite combination as well (Mueller et al., 2002). When injecting ERα knockout epithelial cells into wildtype stroma, that there was no epithelial outgrowth when compared to control, which suggested that epithelial ERα is required for epithelial outgrowth in the mammary gland (Mueller et al., 2002). This finding was later confirmed with a conditional epithelial ERα knockout (Feng et al., 2007). When injecting wildtype epithelial cells into an ERα knockout stroma, there was again no epithelial outgrowth when comparing to control, suggesting that stromal ERα is also required for epithelial outgrowth in the mammary gland (Mueller et al., 2002). Both studies demonstrated the critical role of stromal ERα (Cunha et al., 1997, Mueller et al., 2002). However, it was later determined that these studies used a hypomorphic ERα knockout (Kos et al., 2002). Herein, we provide data that mesenchymal deletion does not prohibit ductal outgrowth. We found that at 12–14 weeks, the mesenchymal ERα knockout mice have a significantly reduced amount of ERα expression in the stromal compartment when compared to control (Fig. 1B–C). However, our deletion is limited to Twist2 expressing cells and does not knockout ERα in all stromal lineages. Additionally, we found that Twist2-cre deleted ERα in the stroma of the female reproductive tract. Although a substantial proportion of stromal cells retained ERα, the uterus and vagina were underdeveloped in the mesenchymal ERα knockout mice (Fig. 2C). ERα in the stromal cells has a crucial role in the functions of the female reproductive tract, including the vagina and uterus (Curtis Hewitt et al., 2000, Hewitt and Korach, 2003, Hewitt et al., 2016, Laronda et al., 2012), therefore it is no surprise that the vaginal epithelium showed abnormal differentiation. Our current study confirms the significant roles of ERα in the mesenchymal cell lineage for proper reproductive tract development.

Role of mesenchymal ERα in in mammary tumorigenesis

There are numerous studies with correlative evidence that BPA signaling occurs through ERα (Hindman et al., 2017, Weber Lozada and Keri, 2011, Wadia et al., 2013, Soto et al.,

2013, Speroni et al., 2017), but no studies have shown that in utero BPA exposure results in BPA signaling through mesenchymal ERα to increase tumorigenesis. Mice that were not exposed to BPA had overlapping tumor initiation and progression outcomes regardless of ERα status, demonstrating mesenchymal ERα is dispensable for tumorigenicity in this model. This result was particularly interesting as there were clear differences in the epithelial content between the ERαΔM mice and controls, and known paracrine signaling mechanisms between the stroma and epithelium influence both development and proliferation. In utero BPA exposure did not lead to a statistically significant decrease in tumor latency compared to the oil controls, although in utero BPA exposure did trend to have a worse outcome with regards to tumor free survival and overall survival compared to vehicle controls (Fig. 4E–F). Similarly, a recent study using this cancer model found mice treated with BPA in the μg/kg · bodyweight ranges (50 or 250 μg/kg · bodyweight), found that only the 250 ug/kg · bodyweight dose led to statistically significant increase in mammary morphogenesis (Ma et al., 2020). Nevertheless, we found that in utero BPA exposure had a statistically significant worse outcome for both tumor free survival and overall survival in mice which had mesenchymal ERα compared to mice that did not have mesenchymal ERα (Fig. 4E–F). This difference indicates that BPA does signal through mesenchymal ERα to alter tumor free- and overall survival results, but further analysis in a cancer model in which BPA has a stronger effect will validate this initial finding.

Conclusions

Herein, we generated a mouse model to test the requirement of mesenchymal ERα for BPA-induced increase in mammary gland tumorigenesis. We found that mesenchymal ERα knockout mice have delayed epithelial elongation. Additionally, mesenchymal ERα is required for proper reproductive tract development and knocking out mesenchymal ERα alters estrogen cycling in these mice. Our model demonstrated that BPA exposed mice trended towards having a worse prognosis in terms of tumor free survival and overall survival. Further, BPA exposed mice with mesenchymal ERα mice have a significantly worse prognosis in terms of tumor free survival and overall survival compared to those without mesenchymal ERα, indicating that BPA has some affect through mesenchymal ERα.

Supplementary Material

Refer to Web version on PubMed Central for supplementary material.

Acknowledgements

We thank The Ohio State University Comprehensive Cancer Center Comparative Pathology and Digital Imaging Shared Resource (CPDISR) for excellent histology support and histopathologic evaluation.

Funding

Research reported in this publication was supported by The Ohio State University Comprehensive Cancer Center, Pelotonia, the National Institutes of Health, National Cancer Institute (P30 CA016058) and National Institutes of Environmental Health sciences (1R01ES032026).

References

2011. National Toxicology Program. Specifications for the Conduct of Studies to Evaluate the Reproductive and Developmental Toxicity of Chemical, Biological and Physical Agents in Laboratory Animals for the National Toxicology Program (NTP).

BANKHEAD P, LOUGHREY MB, FERNÁNDEZ JA, DOMBROWSKI Y, MCART DG, DUNNE PD, MCQUAID S, GRAY RT, MURRAY LJ, COLEMAN HG, JAMES JA, SALTO-TELLEZ M & HAMILTON PW 2017. QuPath: Open source software for digital pathology image analysis. Sci Rep, 7, 16878. [PubMed: 29203879]

BOCCHINFUSO WP & KORACH KS 1997. Mammary gland development and tumorigenesis in estrogen receptor knockout mice. J Mammary Gland Biol Neoplasia, 2, 323–34. [PubMed: 10935020]

BUCHANAN DL, KURITA T, TAYLOR JA, LUBAHN DB, CUNHA GR & COOKE PS 1998. Role of stromal and epithelial estrogen receptors in vaginal epithelial proliferation, stratification, and cornification. Endocrinology, 139, 4345–52. [PubMed: 9751518]

BUCHANAN DL, SETIAWAN T, LUBAHN DB, TAYLOR JA, KURITA T, CUNHA GR & COOKE PS 1999. Tissue compartment-specific estrogen receptor-alpha participation in the mouse uterine epithelial secretory response. Endocrinology, 140, 484–91. [PubMed: 9886861]

BYERS SL, WILES MV, DUNN SL & TAFT RA 2012. Mouse estrous cycle identification tool and images. PLoS One, 7, e35538. [PubMed: 22514749]

CALIGIONI CS 2009. Assessing reproductive status/stages in mice. Curr Protoc Neurosci, Appendix 4, Appendix 4I.

COOKE PS, BUCHANAN DL, YOUNG P, SETIAWAN T, BRODY J, KORACH KS, TAYLOR J, LUBAHN DB & CUNHA GR 1997. Stromal estrogen receptors mediate mitogenic effects of estradiol on uterine epithelium. Proc Natl Acad Sci U S A, 94, 6535–40. [PubMed: 9177253]

CORA MC, KOOISTRA L & TRAVLOS G 2015. Vaginal Cytology of the Laboratory Rat and Mouse: Review and Criteria for the Staging of the Estrous Cycle Using Stained Vaginal Smears. Toxicol Pathol, 43, 776–93. [PubMed: 25739587]

COUSE JF, CURTIS SW, WASHBURN TF, LINDZEY J, GOLDING TS, LUBAHN DB, SMITHIES O & KORACH KS 1995. Analysis of transcription and estrogen insensitivity in the female mouse after targeted disruption of the estrogen receptor gene. Mol Endocrinol, 9, 1441–54. [PubMed: 8584021]

CUNHA GR, YOUNG P, HOM YK, COOKE PS, TAYLOR JA & LUBAHN DB 1997. Elucidation of a role for stromal steroid hormone receptors in mammary gland growth and development using tissue recombinants. J Mammary Gland Biol Neoplasia, 2, 393–402. [PubMed: 10935027]

CURTIS HEWITT S, COUSE JF & KORACH KS 2000. Estrogen receptor transcription and transactivation: Estrogen receptor knockout mice: what their phenotypes reveal about mechanisms of estrogen action. Breast Cancer Res, 2, 345–52. [PubMed: 11250727]

DART DA, WAXMAN J, ABOAGYE EO & BEVAN CL 2013. Visualising androgen receptor activity in male and female mice. PLoS One, 8, e71694. [PubMed: 23940781]

FENG Y, MANKA D, WAGNER KU & KHAN SA 2007. Estrogen receptor-alpha expression in the mammary epithelium is required for ductal and alveolar morphogenesis in mice. Proc Natl Acad Sci U S A, 104, 14718–23. [PubMed: 17785410]

FRIEDRICHS N, STEINER S, BUETTNER R & KNOEPFLE G 2007. Immunohistochemical expression patterns of AP2alpha and AP2gamma in the developing fetal human breast. Histopathology, 51, 814–23. [PubMed: 18042070]

GUY CT, WEBSTER MA, SCHALLER M, PARSONS TJ, CARDIFF RD & MULLER WJ 1992. Expression of the neu protooncogene in the mammary epithelium of transgenic mice induces metastatic disease. Proc Natl Acad Sci U S A, 89, 10578–82. [PubMed: 1359541]

HASLAM SZ & NUMMY KA 1992. The ontogeny and cellular distribution of estrogen receptors in normal mouse mammary gland. J Steroid Biochem Mol Biol, 42, 589–95. [PubMed: 1637722]

HATCH EE, PALMER JR, TITUS-ERNSTOFF L, NOLLER KL, KAUFMAN RH, MITTENDORF R, ROBBOY SJ, HYER M, COWAN CM, ADAM E, COLTON T, HARTGE P & HOOVER RN

1998. Cancer risk in women exposed to diethylstilbestrol in utero. JAMA, 280, 630–4. [PubMed: 9718055]

HEWITT SC & KORACH KS 2003. Oestrogen receptor knockout mice: roles for oestrogen receptors alpha and beta in reproductive tissues. Reproduction, 125, 143–9. [PubMed: 12578528]

HEWITT SC, WINUTHAYANON W & KORACH KS 2016. What's new in estrogen receptor action in the female reproductive tract. J Mol Endocrinol, 56, R55–71. [PubMed: 26826253]

HINDMAN AR, MO XM, HELBER HL, KOVALCHIN CE, RAVICHANDRAN N, MURPHY AR, FAGAN AM, ST JOHN PM & BURD CJ 2017. Varying Susceptibility of the Female Mammary Gland to In Utero Windows of BPA Exposure. Endocrinology, 158, 3435–3447. [PubMed: 28938483]

HIREMATH M, DANN P, FISCHER J, BUTTERWORTH D, BORAS-GRANIC K, HENS J, VAN HOUTEN J, SHI W & WYSOLMERSKI J 2012. Parathyroid hormone-related protein activates Wnt signaling to specify the embryonic mammary mesenchyme. Development, 139, 4239–49. [PubMed: 23034629]

HOOVER RN, HYER M, PFEIFFER RM, ADAM E, BOND B, CHEVILLE AL, COLTON T, HARTGE P, HATCH EE, HERBST AL, KARLAN BY, KAUFMAN R, NOLLER KL, PALMER JR, ROBBOY SJ, SAAL RC, STROHSNITTER W, TITUS-ERNSTOFF L & TROISI R 2011. Adverse health outcomes in women exposed in utero to diethylstilbestrol. N Engl J Med, 365, 1304–14. [PubMed: 21991952]

KEELING JW, OZER E, KING G & WALKER F 2000. Oestrogen receptor alpha in female fetal, infant, and child mammary tissue. J Pathol, 191, 449–51. [PubMed: 10918221]

KORACH KS, COUSE JF, CURTIS SW, WASHBURN TF, LINDZEY J, KIMBRO KS, EDDY EM, MIGLIACCIO S, SNEDEKER SM, LUBAHN DB, SCHOMBERG DW & SMITH EP 1996. Estrogen receptor gene disruption: molecular characterization and experimental and clinical phenotypes. Recent Prog Horm Res, 51, 159–86; discussion 186–8. [PubMed: 8701078]

KOS M, DENGER S, REID G, KORACH KS & GANNON F 2002. Down but not out? A novel protein isoform of the estrogen receptor alpha is expressed in the estrogen receptor alpha knockout mouse. J Mol Endocrinol, 29, 281–6. [PubMed: 12459030]

KURITA T, COOKE PS & CUNHA GR 2001. Epithelial-stromal tissue interaction in paramesonephric (Mullerian) epithelial differentiation. Dev Biol, 240, 194–211. [PubMed: 11784056]

KURITA T, LEE KJ, COOKE PS, TAYLOR JA, LUBAHN DB & CUNHA GR 2000. Paracrine regulation of epithelial progesterone receptor by estradiol in the mouse female reproductive tract. Biol Reprod, 62, 821–30. [PubMed: 10727249]

LARONDA MM, UNNO K, BUTLER LM & KURITA T 2012. The development of cervical and vaginal adenosis as a result of diethylstilbestrol exposure in utero. Differentiation, 84, 252–60. [PubMed: 22682699]

MA Z, PARRIS AB, HOWARD EW, DAVIS M, CAO X, WOODS C & YANG X 2020. In Utero Exposure to Bisphenol a Promotes Mammary Tumor Risk in MMTV-Erbb2 Transgenic Mice Through the Induction of ER-erbB2 Crosstalk. Int J Mol Sci, 21.

MALLEPELL S, KRUST A, CHAMBON P & BRISKEN C 2006. Paracrine signaling through the epithelial estrogen receptor alpha is required for proliferation and morphogenesis in the mammary gland. Proc Natl Acad Sci U S A, 103, 2196–201. [PubMed: 16452162]

MATOUSKOVA K, SZABO GK, DAUM J, FENTON SE, CHRISTIANSEN S, SOTO AM, KAY JE, CARDONA B & VANDENBERG LN 2022. Best practices to quantify the impact of reproductive toxicants on development, function, and diseases of the rodent mammary gland. Reprod Toxicol, 112, 51–67. [PubMed: 35764275]

MUELLER SO, CLARK JA, MYERS PH & KORACH KS 2002. Mammary gland development in adult mice requires epithelial and stromal estrogen receptor alpha. Endocrinology, 143, 2357–65. [PubMed: 12021201]

MULLER WJ, ARTEAGA CL, MUTHUSWAMY SK, SIEGEL PM, WEBSTER MA, CARDIFF RD, MEISE KS, LI F, HALTER SA & COFFEY RJ 1996. Synergistic interaction of the Neu proto-oncogene product and transforming growth factor alpha in the mammary epithelium of transgenic mice. Mol Cell Biol, 16, 5726–36. [PubMed: 8816486]

NACCARATO AG, VIACAVA P, VIGNATI S, FANELLI G, BONADIO AG, MONTRUCCOLI G & BEVILACQUA G 2000. Bio-morphological events in the development of the human female mammary gland from fetal age to puberty. Virchows Arch, 436, 431–8. [PubMed: 10881736]

PALMER JR, WISE LA, HATCH EE, TROISI R, TITUS-ERNSTOFF L, STROHSNITTER W, KAUFMAN R, HERBST AL, NOLLER KL, HYER M & HOOVER RN 2006. Prenatal diethylstilbestrol exposure and risk of breast cancer. Cancer Epidemiol Biomarkers Prev, 15, 1509–14. [PubMed: 16896041]

PARMAR H & CUNHA GR 2004. Epithelial-stromal interactions in the mouse and human mammary gland in vivo. Endocr Relat Cancer, 11, 437–58. [PubMed: 15369447]

ROBINSON GW 2007. Cooperation of signalling pathways in embryonic mammary gland development. Nat Rev Genet, 8, 963–72. [PubMed: 18007652]

SMALLEY MJ 2010. Isolation, culture and analysis of mouse mammary epithelial cells. Methods Mol Biol, 633, 139–70. [PubMed: 20204626]

ŠOŠIĆ D, RICHARDSON JA, YU K, ORNITZ DM & OLSON EN 2003. Twist regulates cytokine gene expression through a negative feedback loop that represses NF-kappaB activity. Cell, 112, 169–80. [PubMed: 12553906]

SOTO AM, BRISKEN C, SCHAEBERLE C & SONNENSCHEIN C 2013. Does cancer start in the womb? altered mammary gland development and predisposition to breast cancer due to in utero exposure to endocrine disruptors. J Mammary Gland Biol Neoplasia, 18, 199–208. [PubMed: 23702822]

SPERONI L, VOUTILAINEN M, MIKKOLA ML, KLAGER SA, SCHAEBERLE CM, SONNENSCHEIN C & SOTO AM 2017. New insights into fetal mammary gland morphogenesis: differential effects of natural and environmental estrogens. Sci Rep, 7, 40806. [PubMed: 28102330]

STANKO JP, EASTERLING MR & FENTON SE 2015. Application of Sholl analysis to quantify changes in growth and development in rat mammary gland whole mounts. Reprod Toxicol, 54, 129–35. [PubMed: 25463529]

STANKO JP & FENTON SE 2017. Quantifying Branching Density in Rat Mammary Gland Whole-mounts Using the Sholl Analysis Method. J Vis Exp.

STERNLICHT MD 2006. Key stages in mammary gland development: the cues that regulate ductal branching morphogenesis. Breast Cancer Res, 8, 201. [PubMed: 16524451]

WADIA PR, CABATON NJ, BORRERO MD, RUBIN BS, SONNENSCHEIN C, SHIODA T & SOTO AM 2013. Low-dose BPA exposure alters the mesenchymal and epithelial transcriptomes of the mouse fetal mammary gland. PLoS One, 8, e63902. [PubMed: 23704952]

WEBER LOZADA K & KERI RA 2011. Bisphenol A increases mammary cancer risk in two distinct mouse models of breast cancer. Biol Reprod, 85, 490–7. [PubMed: 21636739]

WESTWOOD FR 2008. The female rat reproductive cycle: a practical histological guide to staging. Toxicol Pathol, 36, 375–84. [PubMed: 18441260]

WETENDORF M, WU SP, WANG X, CREIGHTON CJ, WANG T, LANZ RB, BLOK L, TSAI SY, TSAI MJ, LYDON JP & DEMAYO FJ 2017. Decreased epithelial progesterone receptor A at the window of receptivity is required for preparation of the endometrium for embryo attachment. Biol Reprod, 96, 313–326. [PubMed: 28203817]

WORMSBAECHER C, HINDMAN AR, AVENDANO A, CORTES-MEDINA M, JONES CE, BUSHMAN A, ONUA L, KOVALCHIN CE, MURPHY AR, HELBER HL, SHAPIRO A, VOYTOVITCH K, KUANG X, AGUILAR-VALENZUELA R, LEIGHT JL, SONG JW & BURD CJ 2020. In utero estrogenic endocrine disruption alters the stroma to increase extracellular matrix density and mammary gland stiffness. Breast Cancer Res, 22, 41. [PubMed: 32370801]

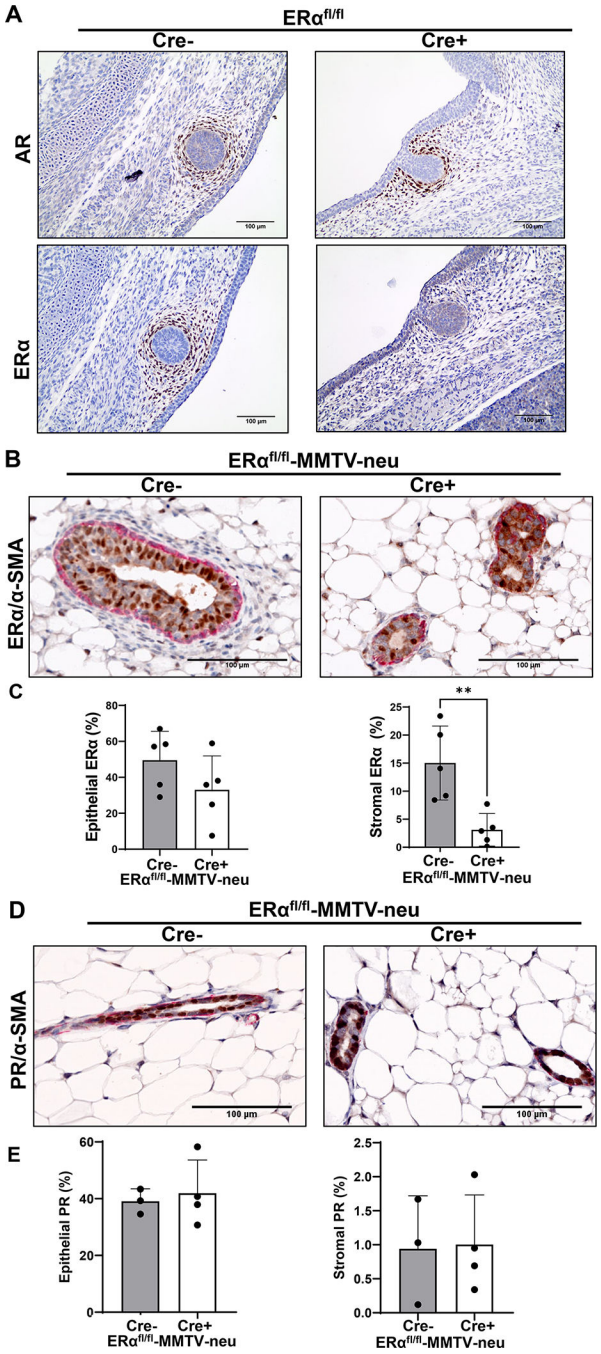

Figure 1. Efficient knockout of mesenchymal ERα in ERαΔM mice.

A To validate mesenchymal ERα knockout in ERαΔM mice, mammary buds were first identified at embryonic day 13.5 (E13.5) by IHC for the androgen receptor (AR) (top). Sequential sections were stained for estrogen receptor alpha (ERα) (bottom). Images taken at 20X magnification. **B** Representative images of IHC of mammary glands from control and mesenchymal ERα knockout ERαΔM-MMTV-neu mice from 12–14 week old mice, dual stained with ERα (brown)/α-SMA (red). Images are at 20X magnification. **C** Graphs show quantification of percentage of ERα positivity in the epithelial compartment (left) and

the stromal compartment (right). Graphed as mean ± standard deviation, each dot represents one mouse, five mice from four litters were assessed in the control group and five mice from five litters were assessed in the ERαΔM-MMTV-neu group. Significance determined by a t-test, p=0.0061. **D** Representative images of IHC of mammary glands from control and mesenchymal ERα knockout ERαΔM-MMTV-neu mice from 12–14 week old mice, dual stained with PR/α-SMA, focused on ductal areas. Images are at 20X magnification. **E** Graphs show quantification of percentage of PR positivity in the epithelial compartment (left) and the stromal compartment (right). Graphed as mean ± standard deviation, each dot represents one mouse, three mice from three litters were assessed in the control group and four mice from three litters were assessed in the ERαΔM-MMTV-neu group.

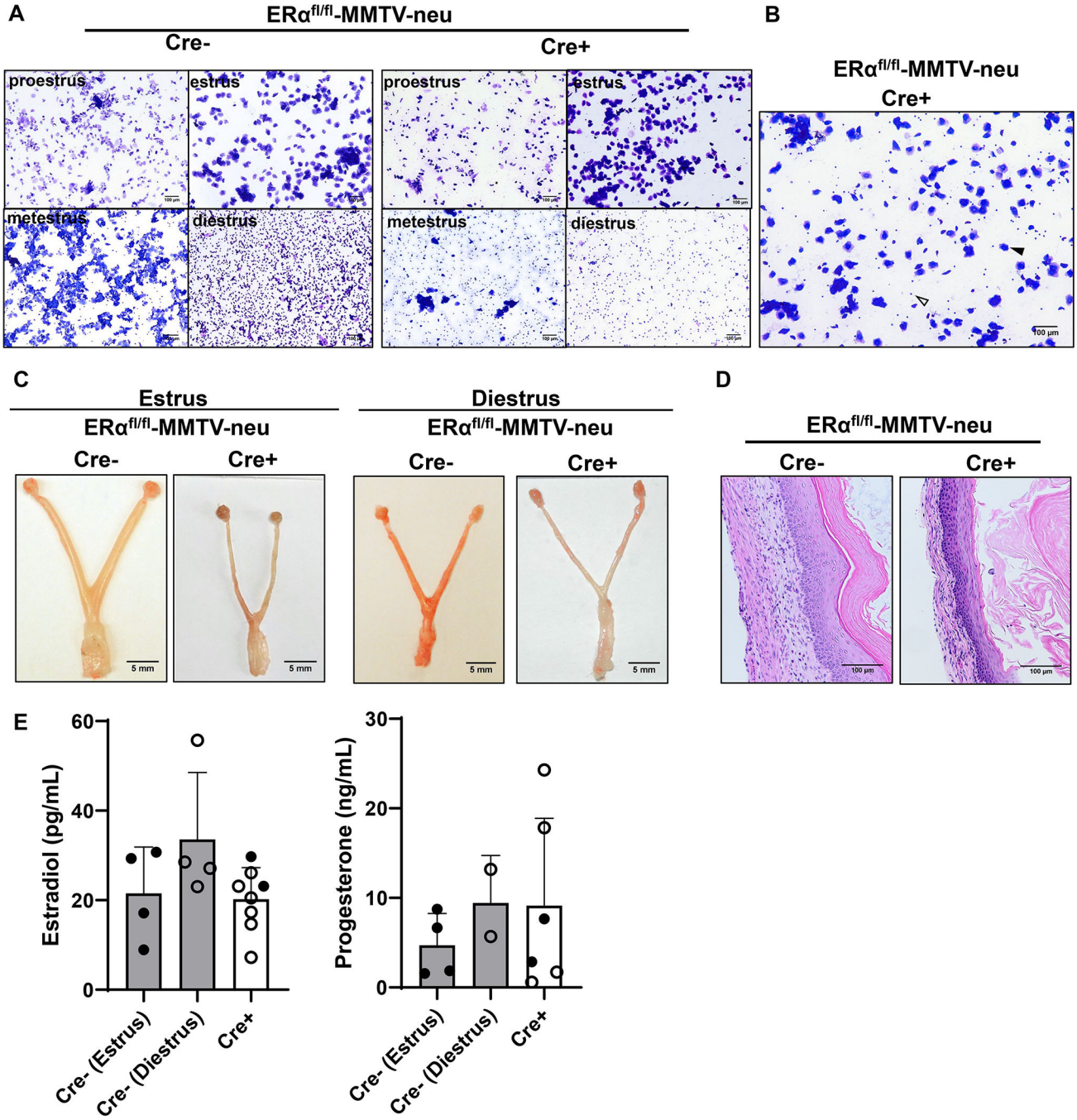

Figure 2. Mesenchymal ERα knockout mice have altered response to estrous cycling.

A Vaginal cytology samples in each stage of estrous cycling from control and ERαΔM-MMTV-neu mice. Images taken at 10X magnification. **B** Reoccurring vaginal cytology sample in ERαΔM-MMTV-neu mice. Image taken at 10X magnification. Filled-in arrow heads indicating squamous epithelial cells and open arrow heads indicating leukocytes. **C** Images of reproductive tract from control and ERαΔM-MMTV-neu mice collected in the estrus stage (left) and in the diestrus stage (right) as measured by vaginal cytology. **D** H&E staining of vaginal sections collected from mice in the estrus stage as measured by vaginal

cytology. Images taken at 20X magnification. **E** Estradiol (left) and progesterone (right) serum levels of control mice collected in both estrus (filled in circles) and diestrus stages (open circles), compared to serum levels from ERαΔM-MMTV-neu mice. ERαΔM-MMTV-neu serum collected from mice in stage closest to estrus per vaginal cytology in closed circles and collected in stage closest identified to diestrus per vaginal cytology in open circles. Graphed as mean ± standard deviation, each dot represents one mouse.

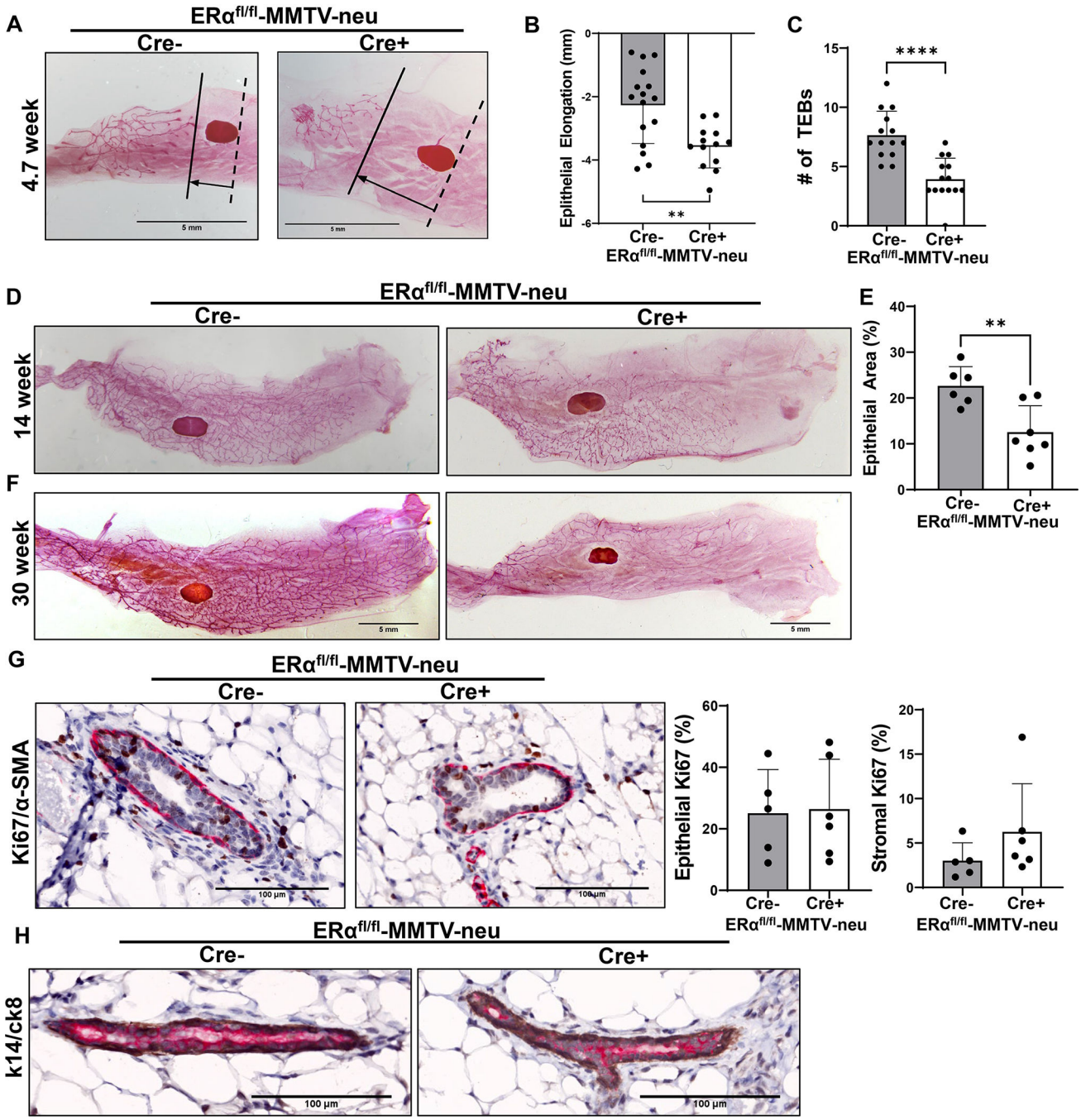

Figure 3. ERαΔM-MMTV-neu have delayed epithelial elongation at 4.7 weeks and reduced epithelial area in adulthood.

A Mammary glands were collected in control and ERαΔM-MMTV-neu mice at 4.7 weeks, whole mounted, and carmine-aluminum stained to look at epithelial elongation. Images taken at 1X magnification. **B** Epithelial elongation was measured in 4.7 week whole mounts by measuring from the lymph node, plus or minus to the most distal point of epithelial elongation in stained mammary whole mounts with quantification graphed to the right. Graphed as mean ± standard deviation, each dot represents one mouse, and mice from

six separate litters were analyzed. Significance determined by a t-test, p=0.0017. **C** The number of terminal end buds was quantified in whole mount images of 4.7 week old mice. Graphed as mean ± standard deviation, each dot represents one mouse, and mice from six separate litters were analyzed. Significance determined by a t-test, p<0.0001. **D** Mammary glands were collected in control and ERαΔM-MMTV-neu mice at about 14 weeks, whole mounted, and stained to look at epithelial area. Images taken at 0.6X magnification. **E** Epithelial area was measured in 14 week whole mounts by measuring the pixels in the epithelium as a percentage of total pixels in the whole mammary fat pad. Graphed as mean ± standard deviation, each dot represents one mouse, and mice from at least five separate litters were analyzed. Significance determined by a t-test, p=0.0045. **E** Whole mounted mammary glands collected at 28–30 weeks of age from control and ERαΔM-MMTV-neu mice. Images taken at 0.6X magnification. **F** Representative images of IHC of mammary glands from control and mesenchymal ERα knockout (ERαΔM-MMTV-neu) mice from adult 14 week old mice, dual stained with Ki67 (brown)/α-SMA (red), focused on ductal areas. Images are at 20X magnification. **G** Graphs show quantification of percentage of Ki67 positivity in the epithelial compartment (left) and the stromal compartment (right). Graphed as mean ± standard deviation, each dot represents one mouse, five mice from five litters were assessed in both groups. **H** Representative images of IHC of mammary glands from control and mesenchymal ER α knockout ERαΔM-MMTV-neu mice from adult 14week old mice, dual stained with k14(brown)/ck8 (red), focused on ductal areas. Images are at 20X magnification.

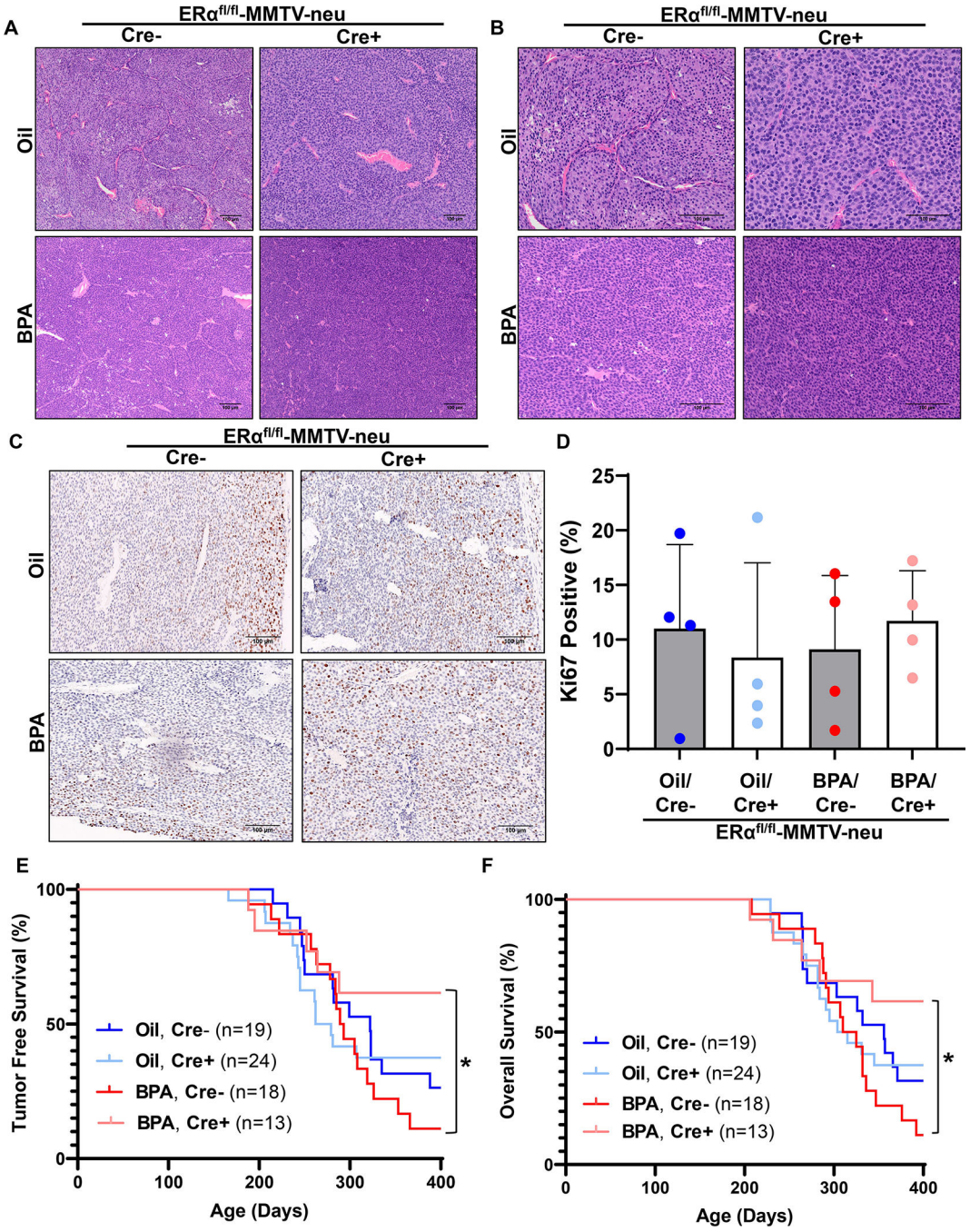

Figure 4. Mesenchymal ERα knockout mice exposed in utero to BPA have better outcomes compared to mice with mesenchymal ERα. A

Tumors from control mice with mesenchymal ERα and mice without mesenchymal ERα (ERαΔM-MMTV-neu) which were exposed in utero to oil or BPA were harvested once reached exclusion criteria and stained with H&E after fixation. Representative images from H&E on tumors, taken at 10X magnification and 20X magnification (**B**). **C** Representative images of Ki67 IHC of tumors from control and ERαΔM-MMTV-neu mice focused on tumor edges. Images are at 20X magnification. **D** Graph shows quantification of percentage

of Ki67 positivity at the tumor edges. Graphed as mean ± standard deviation, each dot represents one mouse, four mice from at least three separate litters were assessed for each group. **E** Kaplan-meier curves graphing tumor free survival (time until observation of first tumor) and overall survival (time until mice reached exclusion) (**F**) Significance determined by a log rank test, each cohort contains mice from at least eight separate litters.